Available online at www.sciencedirect.com
SCIENCE DIRECT®
Journal of Solid State Chemistry 177 (2004) 3522–3528
JOURNAL OF SOLID STATE CHEMISTRY
www.elsevier.com/locate/jssc

Facile solvent-free synthesis of pure-phased AlN nanowhiskers at a low temperature

Changzheng Wu[a,b], Qing Yang[a,b,*], Chao Huang[b], Dong Wang[b], Ping Yin[b], Tanwei Li[b], Yi Xie[a,b,*]

[a]*Nano-materials and Nano-chemistry, Hefei National Laboratory for Physical Sciences at Microscale, Hefei, Anhui 230026, China*
[b]*Department of Chemistry, University of Science and Technology, Hefei, Anhui 230026, China*

Received 29 April 2004; received in revised form 11 June 2004; accepted 21 June 2004
Available online 12 August 2004

Abstract

Pure hexagonal aluminum nitride (AlN) nanowhiskers have been successfully synthesized by directly reacting $AlCl_3$ with NaN_3 in non-solvent system at the low temperature of 450 °C for 24 h. The obtained products are characterized by X-ray diffraction, field emission scanning electron microscopy, transmission electron microscopy, high-resolution transmission electron microscopy and selected area electron diffraction, which show that the obtained products are hexagonal phase AlN nanowhiskers with width from 10 to 80 nm and length up to several micrometers. The influencing factors of the formation of AlN nanowhiskers were discussed and a possible growth mechanism for AlN nanowhiskers was proposed. Additionally, the study on the corresponding optical properties and catalytic properties is also carried out.

1. Introduction

Because the amount of thermal energy produced per unit area during operation is greatly increasing as a result of miniaturization of high-power electronic devices, many efforts have been put on these materials, which can dissipate heat rapidly and then avoid electronic or mechanical failure [1]. Aluminum nitride (AlN) is an important thermal management material for silicon-based electronics due to its very high thermal conductivity ($320\,W\,m^{-1}\,K^{-1}$), low coefficient of thermal expansion ($4.3\times10^{-6}\,K^{-1}$) that matches well with that of silicon, and high mechanical strength [2]. In addition, AlN is an insulator with a large band gap ($E_g = 6.4$ eV), high resistivity ($>10^{11}\,\Omega$ m), and low dielectric constant (8.6) [3]. Thus, it has attracted extensive interest for applications as electrical packaging materials and as components in structural composites [4]. Other applications for this material include UV photo detectors, pressure sensors, thermal radiation sensors, field-effect transistors [5], and catalysts [6]. Especially, AlN nanowhiskers and nanowires have attracted much attention because their perfect or near-perfect crystal structures are supposed to have higher thermal conductivity than ordinary polycrystalline AlN ceramics [7], and they could provide better reinforcement in the composites [8]. AlN whiskers or fibers have been used to optimize the thermal properties of polymer composites for electronic packaging [9].

There is a challenging for new synthetic approaches to pure-phased AlN and other nitrides, because most current methods require complicated equipment and/or high temperatures. Syntheseses of AlN often involve processes with complex equipment, such as ion beam evaporation or DC arc plasma, which forces aluminum ingots to react with ammonia or nitrogen gas under

*Corresponding authors. Department of Chemistry, The University of Science and Technology, No. 96, Jinzhai Road, Hafei City, Anhui Province 230026, China. Tel.: +86-551-360-3987; fax: +86-551-360-3987.
E-mail addresses: qyoung@ustc.edu.cn (Q. Yang), yxielab@ustc.edu.cn (Y. Xie).

0022-4596/$ - see front matter © 2004 Elsevier Inc. All rights reserved.
doi:10.1016/j.jssc.2004.06.035

extreme conditions. Other extensively used methods to fabricate AlN in industry are carbothermal reduction and nitridation of α-alumina [10], and direct nitridation of Al powders or nano-Al [11]. And these methods usually require a reaction temperature of over 1100 K or the introduction of the templates (carbon nanotubes, etc.), which may introduce heterogeneous impurities and increase the production cost. In contrast to numerous literatures published on the preparation of AlN nanocrystals, only a few studies have been focused on the formation of AlN at relative low temperatures. For example, Ohhashi et al. synthesized AlN powders by the reaction of ammonia with a mixture of aluminum chloride vapor species ($AlCl_x$; $x = 1$, 2, and 3) in a flow-tube reactor at 720–920 °C, and the produced particle sizes were in the range of 200–400 nm [12]. Qian et al. reported the synthesis of AlN using Al and NH_4Cl as reactants at 580 °C and the product is spherical particles with average size of 6 nm [13]. Thus, the most challenging problem of synthesizing pure-phased AlN nanowiskers at the low temperatures is how to control both the phase and the morphology of products. Herein, we report a simple chemical route to prepare pure-phased AlN with whisker morphology by using $AlCl_3$ as Al-source and NaN_3 as N-source in the non-solvent system at the low temperature of 450 °C for 24 h. The whole process can be formulated as follows:

$$AlCl_3 + 3NaN_3 \rightarrow AlN + 3NaCl + 4N_2. \quad (1)$$

Some fascinating features are described in the present work: (i) AlN nanowhiskers have been successfully prepared at 450 °C, which is much lower than the temperature used in those traditional methods. (ii) The as-obtained AlN are of pure phase. (iii) The nanowhiskers in the final products are high quality, and the yield of the as-obtained AlN nanowhiskers reaches 70–75%. (iv) In addition, the study on the catalytic effect of the as-prepared AlN nanowhiskers, such as on the condensation of acetone, has been tentatively carried out.

2. Experimental section

2.1. Synthesis of hexagonal AlN nanowhiskers

Details of a typical experiment are as follows: Appropriate amounts of $AlCl_3$ (2 g, 15 mmol) and NaN_3 (3 g, 50 mmol) were put into a stainless steel autoclave of 20 ml capacity. All manipulations were carried out in a dry glove box with Ar gas flowing. The autoclave was sealed and maintained at 450 °C for 24 h and then cooled to room temperature. After the reaction was completed, the resulting gray-white product was filtered, washed with absolute ethanol and 0.5 M HCl to remove byproducts, and then dried at 60 °C in air. The obtained gray-white powders were collected for the following characterization. For comparison, a stoichiometric mixture of 15 mmol $AlCl_3$ and various nitrogen source ($NaNH_2$, NH_4Cl, Mg_3N_2) were also investigated at different temperatures in the current work (see Table 1).

2.2. Study the catalytic effect of AlN nanowhiskers on acetone

Two millimoles as-obtained AlN nanowhiskers (obtained at 450 °C for 24 h) and 10 mL acetone were simultaneously added into autoclave with capacity of 15 mL. After the air had been expelled with nitrogen of high purity (99.999%), the autoclave was sealed and maintained at 150 °C for 12 h. A yellow solution was obtained and further characterized by GC–MS. In order to compare the catalytic effect of AlN with Al_2O_3, similar

Table 1
Experimental conditions and results of reaction of Al sources (Al, $AlCl_3$) with various nitrogen sources ($NaNH_2$, NH_4Cl, Mg_3N_2) in the non-solvent system

Reactants	Condition	Products	Morphologies
$AlCl_3 + NaN_3$	<300 °C	No products	
	350 °C	Crystallized hexagonal AlN	Particles, 10–30 nm
	450 °C	Crystallized hexagonal AlN	Nanowhiskers (75%)
	550 °C	Crystallized hexagonal AlN	Aggregated particles, 30–1000 nm
$AlCl_3 + NaNH_2$	<450 °C	No products	
	500 °C	Crystallized hexagonal AlN	Particles, 10–40 nm
$AlCl_3 + Mg_2N_3$	<550 °C	No products	
	600 °C	Crystallized hexagonal AlN	Particles, 10–60 nm
$AlCl_3 + NH_4Cl$	<550 °C	No products	
	600 °C	Crystallized hexagonal AlN	Particles, 20–50 nm
$Al + NaN_3$	Up to 650 °C	No products	

procedure was carried out by the additive of 1 mmol nanosized Al_2O_3 (same molar content of Al compared with AlN, prepared by the reported literature [14]).

2.3. Characterization

The samples were characterized by X-ray powder diffraction (XRD) with a Japan Rigaku D/max rA X-ray diffractometer equipped with graphite monochromatized high-intensity Cu-$K\alpha$ radiation ($\lambda = 1.54178$ Å). X-ray photoelectron spectroscopy (XPS) measurements were performed on a VGESCALAB MKII X-ray photoelectron spectrometer with an exciting source of Mg$K\alpha = 1253.6$ eV. The transmission electron microscopy (TEM) images were performed with a Hitachi Model H-800 instrument with a tungsten filament, using an accelerating voltage of 200 kV. The field emission scanning electron microscopy (FE-SEM) images were taken on a JEOL JSM-6700F SEM. The electron diffraction (ED) patterns and high-resolution transmission electron microscopy (HRTEM) images were carried out on a JEOL-2010 TEM at an acceleration voltage of 200 KV. FT-IR absorption spectra were performed with a Nicolet FT-IR-170SX spectrometer in the range of 500–4000 cm^{-1} at room temperature, with the sample in a KBr disk. The Raman spectra were recorded at room temperature on a LABRAM-HR Confocal Laser MicroRaman spectrometer. GC–MS were recorded on a Finnigan GC-MS Spectrometer.

3. Results and discussion

3.1. Composition and morphology of the AlN nanowhiskers

The panoramic morphologies of the obtained product (shown in Fig. 1a) are examined by FE-SEM, in which the solid sample is mounted on a copper mesh without any dispersion treatment. The results indicate that the product consists of nanowhiskers with diameters of 10–60 nm on average and aspect ratios (length/diameter) of 20 to >100. The proportion of nanowhiskers in the product is above 75% and their yield is about 35% based on the original reagents. Careful observations show that there exist relatively straight nanowhiskers with coexistence of the twisted, sheet-like whiskers. TEM images at different magnifications (Fig. 1b–c) show the typical relatively straight nanowhiskers. The enlarged TEM image (Fig. 1c) clearly indicates the well-defined geometry of the as-obtained product. More details about the structure of as-obtained nanowhiskers were investigated by high-resolution transmission electron microscopy (HRTEM) (Fig. 1d). The distance of 0.249 nm between the two lattices is in agreement with the spacing d_{002} of *h*-AlN. The ED pattern (the inset in Fig. 1d) indicates that the whiskers are grown along [100] direction. The proportion of straight, single crystalline nanowhiskers is about 40–50% in the product. Besides the straight, single-crystal whiskers, there exist some twisted, sheet-like polycrystalline whiskers in the product (Fig. 1e). Careful observation clearly show the existence of sheet-like morphology (Fig. 1f) and twisted structures (Fig. 1g). From SEM and TEM images, the proportion of sheet-like whiskers could be estimated to be about 20–25%. Typical sheet-like whiskers can be shown in Fig. 1e with diameters from 20 to 100 nm and length up to several micrometers.

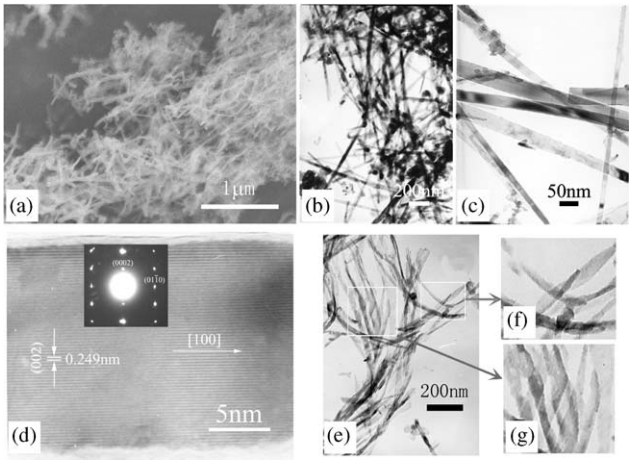

Fig. 1. (a) Typical FE-SEM image of the obtained products. (b) and (c) Low magnification and high magnification TEM images of the relative straight nanowhiskers. (d) HRTEM image of a nanowhisker (inset is the corresponding SAED pattern). (e) and (f) Typical TEM images of fibrous and sheet-like AlN morphologies (e), and the corresponding magnification TEM images, which show the sheet-like morphology (f) and twisted structures (g).

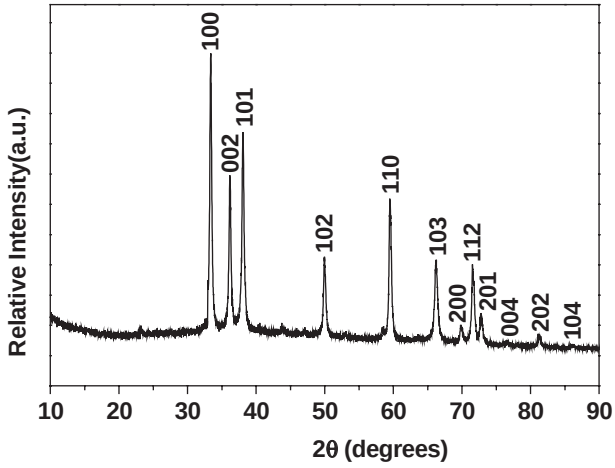

Fig. 2. XRD pattern of the as-prepared AlN nanowhiskers. Miller indices of hexagonal AlN are placed above the corresponding peaks.

The X-ray diffraction (XRD) pattern of the as-prepared gray-white product is shown in Fig. 2. All

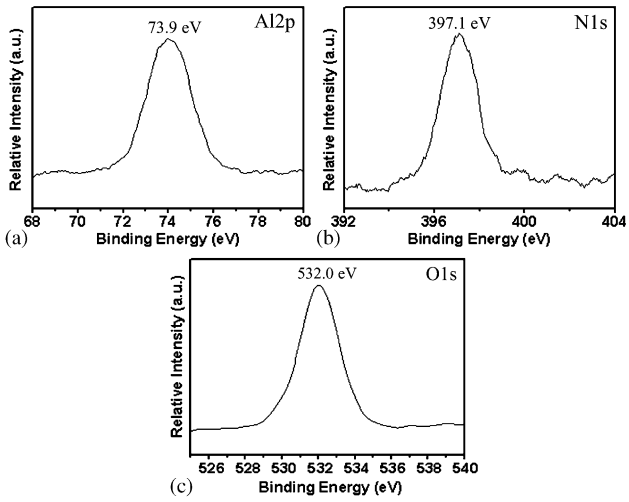

Fig. 3. XPS analysis of as-prepared *h*-AlN.

the reflection peaks could be indexed as hexagonal-phase AlN (*h*-AlN) with constants of $a = 3.10$ and $c = 4.96$ Å, which are consistent with the reported values of *h*-AlN ($a = 3.11$ Å, $c = 4.98$ Å) (JCPDS, No. 25-1133), indicating that the gray-white product is *h*-AlN. No other noticeable peaks introduced by impurities are observed in the XRD patterns. Further evidence for purity and composition of the sample is obtained by XPS measurements. The survey spectrum indicates the presence of Al and N as well as C from the reference and O impurity from absorbed gaseous molecules and the absence of any impurity such as Cl or Na. Higher resolution spectra are also recorded in the Al 2*p* and N 1*s* regions. The peak cores at 73.9 and 397.1 eV corresponded to Al 2*p* and N 1*s*, respectively (shown in Figs. 3a and b), which were close to the reported binding energies [15]. In Fig. 3c, we can see that the O 1*s* profile appears as a single symmetric peak centered at 532.0 eV, which can be attributed to chemisorbed oxygen [16]. On the other hand, the presence of O^{2-} in Al_2O_3 would give rise to asymmetry in the left part of the peaks centered at 531.0 eV [17], indicating O in the survey spectrum is the absorbed gaseous oxygen instead of the O^{2-} in Al_2O_3. By measuring peak areas of N and Al cores, the ratio of N/Al was calculated to be 0.92 and close to chemical stoichiometry. The statistical counting deviation in XPS measurement is usually 3–5 at%. Thus, this product can be formulated as AlN. The level of impurities is thus lower than the resolution limit of XPS (1 at%).

3.2. Formation mechanism for h-AlN

Our approach to *h*-AlN nanostructures is essentially based on the reaction between $AlCl_3$ and NaN_3. And it is known that the thermal decomposition of NaN_3 proceeds according to the overall equation: $2NaN_3 \rightarrow 3N_2 + 2Na$ up to the thermal decomposition temperature of NaN_3 (330 °C) [18]. A previous report on the details of the reaction indicated that nitrogen atoms could be generated from this decomposition process [19]. In our experiments, we may prefer a reduction-nitridation route to ionic metathesis pathway to AlN. According to free energy calculations, Eq. (4) is thermodynamically spontaneous and highly exothermic ($\Delta_r G^\circ = -523.5\,\mathrm{kJ\,mol^{-1}}$, $\Delta_r H^\circ = -529.4\,\mathrm{kJ\,mol^{-1}}$) [20]. Therefore, the formation of aluminium powder is possible, which is somewhat like the synthesis of diamond powder through the reduction of CCl_4 by metallic Na [21]. At the elevated synthetic temperature, $AlCl_3$ and Na are in the vapor and liquid phase ($AlCl_3$: subl. of 181 °C, Na: m.p. of 98 °C) [20], respectively, so the initiating reduction reaction was carried out in the form of vapor–liquid surface reaction. Once the reduction reaction is initiated, the heat generated in the process is sufficient to melt Al and the byproduct NaCl (Al: mp of 660 °C, NaCl: mp of 801 °C), to vaporize the reactant Na (Na, bp of 890 °C) [20]. Thus, the reduction reaction proceeds probably in a vapor-phase of $AlCl_3$ and Na, which allows for a rapid reduction and in turn generates more heat and melts more byproduct. The newly formed Al liquid droplets are so active that they can directly react with the activated N atoms in the NaCl molten flux. The formation process might be illustrated as follows:

$$N_3^- \rightarrow N_2 + N + e + \text{energy}, \tag{2}$$

$$Na^+ + e \rightarrow Na, \tag{3}$$

$$AlCl_3 + 3Na \rightarrow Al + 3NaCl + \text{energy}, \tag{4}$$

$$Al + N \rightarrow AlN. \tag{5}$$

One direct evidence for Al participating in the reaction as an intermediate reactant is that at the shorter time of 4 h, there are the coexistence of AlN and Al in the final products washed by ethanol and dilute HCl. The corresponding XRD pattern is shown in Fig. 4,

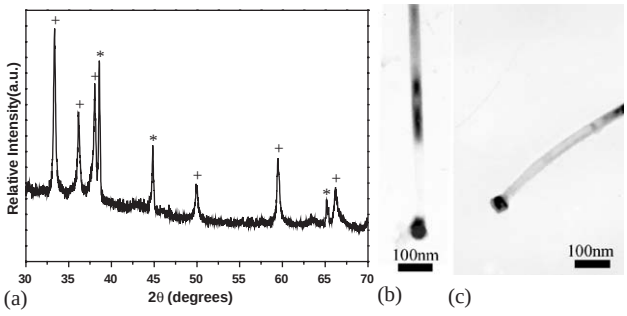

Fig. 4. (a) XRD pattern of the products obtained at 450 °C at the shorter time of 4 h. (b) and (c) AlN (signal +) and Al (signal *). Corresponding TEM images showing two typical growing nanowhiskers of AlN, in which the globule tops can be seen clearly.

in which the reflections have been attributed to two components, AlN with the wurtzite structure (signal +), and Al with cubic structure (signal *). Additionally, comparable experiments with different nitrogen source were also studied in the current work and the results were summarized in Table 1, from which it can be found that both the exothermicity of salt formation and high pressure in the autoclave seem indispensable to the formation of AlN nanocrystals at the low temperature in this system. When NH_4Cl was used, the formula can be shown as follows:

$$AlCl_3 + NH_4Cl \rightarrow AlN + 4HCl. \quad (6)$$

Although the byproducts HCl in this approach could provide enough pressure in the autoclave (about 8 MPa estimated by the idea gas law), which is close to the value of the pressure produced by the reaction between $AlCl_3$ and NaN_3, there are yet no crystalline AlN obtained until the temperature was elevated to 600 °C. The possible reason might be that there is no formation of the ionic salt (such as NaCl) in the final products, which is usually regarded as the favorable driving force for the formation of the final products in solid-state reactions [22]. On the other hand, when Mg_3N_2 was introduced, although the ionic salt will be formed in this case, the crystalline AlN can only be obtained at the temperature of higher than 600 °C due to the absence of the high pressure produced by the gaseous byproducts produced in the reaction process according to the reaction formula:

$$2AlCl_3 + Mg_3N_2 \rightarrow 2AlN + 3MgCl_2. \quad (7)$$

In the case of $NaNH_2$, the formula can be shown as follows according to previous literatures [23]:

$$3NaNH_2 \rightarrow Na_3N + 2NH_3, \quad (8)$$

$$AlCl_3 + Na_3N \rightarrow AlN + 3NaCl. \quad (9)$$

The lowest temperature for crystalline AlN by the reaction between $AlCl_3$ and $NaNH_2$ is 500 °C, which is lower than the temperature obtained by the reaction between $AlCl_3$ and Mg_3N_2 or $AlCl_3$ and NH_4Cl. This may be result from the existence of both ionic salt (NaCl) and the gaseous pressure produced in the formation process (about 4 MPa estimated by the ideal gas law).

3.3. Growth mechanism of AlN nanowhiskers

Here, we prefer the vapor–liquid–solid (VLS) mechanism, rather than the other two well-known whisker-growth mechanisms, namely, solution–liquid–solid (SLS), vapor–solid (VS) to function for the formation of AlN nanowhiskers under the present conditions. Moreover, it is worth noting that there are liquid globules, which is inherent to the VLS mechanism, were found on the tip of the nanowhiskers in the products after reacting 4 h (shown in Figs. 4B and C). This fact suggests that the VLS mechanism was dominant in the AlN nanowhisker synthesis. As described above, the large amount of heat generated in this process can result in a high temperature molten NaCl–Al flux. The surface of the molten NaCl–Al flux may has a large accommodation coefficient and is therefore a preferred site for deposition of the activated vapor phase reactant activated N atoms, which can benefit the VLS nucleation for AlN. Meanwhile, the molten NaCl–Al flux may also play a role in facilitating the growth of AlN nanowhiskers. Since crystal growth involves the exchange of atoms at the growth front planes, the high-temperature molten NaCl–Al flux could keep impinging atoms from being dislodged by thermal diffusions and thermal vibrations, and thus enhance the nanowhisker growth. The whole formation process can be shown in Scheme 1. A feature of this synthetic route is the high pressure in the autoclave, coming from the produced N_2 in the reaction procedure (about 8 MPa estimated by the idea gas law), which favors the formation of crystalline AlN at relatively low temperature. Additionally, the byproducts N_2 in this approach could provide the non-oxygen environment in the sealed system, which ensures the purity of the final products.

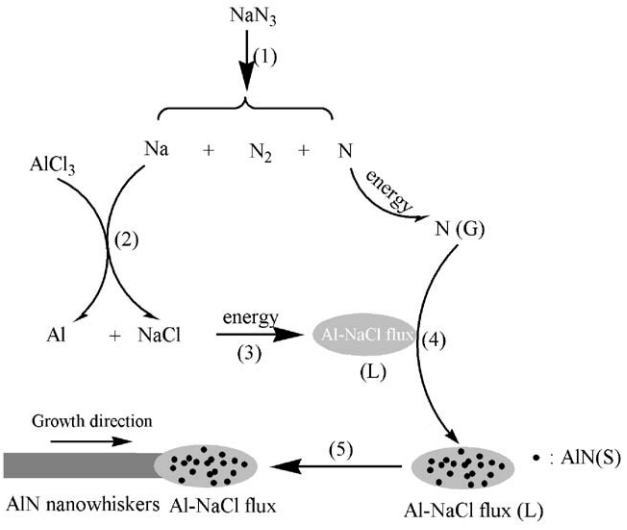

Scheme 1. Schematic illustration for the growth of AlN nanowhiskers under a vapor–liquid–solid model: (1) at an elevated temperature, NaN_3 decompose to produce Na, N_2 and activated N atoms. (2) The reduction reaction proceeds and generates more heat, Al and ionic salt (NaCl). (3) The large amount of heat generated in this process results in a high temperature molten NaCl–Al flux. (4) The newly formed Al liquid droplets directly react with the activated N atoms to produce AlN particles in the NaCl molten flux. (5) The surface of the molten NaCl–Al flux may has a large accommodation coefficient and is therefore a preferred site for deposition of the activated vapor phase reactant activated N atoms to form AlN particles. After the flux becomes supersaturated with AlN, AlN nanowhiskers growth occurs by precipitation at the solid–liquid interface (G: gas; L: liquid; S: solid).

To investigate the effect of reaction conditions on the formation of AlN nanowhiskers, a series of relevant experiments were carried out through similar processes. It is obvious that the reaction temperature played a critical role in the formation of AlN nanowhiskers. Lower temperature than 300 °C could not initiate the reactions. AlN nanowhiskers became observable when the reaction temperature is higher than 400 °C. It is found that the appropriate temperature for the growth of AlN nanowhiskers is 400–500 °C. At the temperature of higher than 550 °C, there are only aggregated AlN particles instead of nanowhiskers could be obtained. Comparable experiments show that both of $AlCl_3$ and NaN_3 seem indispensable to the formation of AlN nanowhiskers in this system. When $AlCl_3$ is substituted by commercial Al, there are no AlN obtained even though the temperature was increased to 650 °C while other experimental parameters were kept constant. And when $NaNH_2$, Mg_3N_2 or NH_4Cl is used as nitrogen-source, there are no fiber-like or flake-like morphologies obtained in the final products (see Table 1).

3.4. Optical characterization of the AlN nanowhiskers

For the FT-IR transmission spectrum (Fig. 5a) of the obtained nanowhiskers, the intense and broad band centered at about 690 cm^{-1} belonging to the Al–N band of nanostructured AlN crystal [24]. Furthermore it should be noted that there are two shoulders at about 630 and 813 cm^{-1} on both sides of the 690 cm^{-1}. The absorption at 630 cm^{-1} is agreement in the TO_2 phonon modes of AlN film [25]. However, the shoulder at 813 cm^{-1} is uncertain and it may be the absorption of the vibration of γ or δ (Al–N_2) at 840 cm^{-1} as reported in films [26]. There are some weak bands in the region of both 1000−1900 and 2400–3500 cm^{-1}, which can be attributed to a very small amount of water, CO_2, and air in the spectrometer path or the surface of the samples [27]. Al–O peaks at 950 or 460 cm^{-1} have not been detected, indicating the high purity of *h*-AlN species in the sample.

Raman Spectroscopy, a powerful experimental technique for the identification and characterization of nanomaterials, could be used to probe the presence of lattice defects in these solids qualitatively [28]. The space group of wurtzite AlN is C_{6v}^4 ($P6_3mc$) with all atoms occupying the C_{3v} sites. The zinc blende structure has only two Raman-active phonons F_2 (TO) and F_2 (LO), while the wurtzite structure has six Raman-active phonons: A_1 (TO), A_1 (LO), E_1 (TO), E_1 (LO), and $2E_2$ [29]. Therefore, the number of peaks observed in the Raman spectra indicates whether the wurtzite phase is present or not. The typical Raman spectrum of the as-prepared nanowhiskers is shown in supporting information. It is seen from typical Raman spectrum of the as-prepared hexagonal nanowhiskers (Fig. 5b), A_1 (TO), E_2 (high), and E_1 (TO) modes present at 610.2, 656.8, 669.0 cm^{-1}, respectively. A rather broad peak centered around 900 cm^{-1} may result from the modes of A_1 (LO) and E_1 (LO). In a word, it could be concluded that the as-prepared AlN nanowhiskers is similar to the crystal AlN [30] in the optical properties, despite its one-dimensional geometry.

3.5. Chemical reactivity of nanosized AlN on acetone condensation

For chemical reactivity of the as-obtained products, it is well known that AlN is generally regarded as a Lewis acid, which can be introduced to the Lewis-acid catalysed organic reactions. It has been reported that nanoscaled AlN can catalyze the polymerization of benzene as a Lewis-acid catalyst [6], and we found that the similar effect can work on acetone condensation. The typical chromatography pattern of the solution indicates that, with the additive of as-obtained nanosized AlN, there were three primary products obtained (middle, Fig. 6a): dimer of acetone (4-methyl-4-hydro-2-pentanone, **1**) and its two dehydrates (4-methyl-3-penten-2-one, **2a**; 4-methyl-4-penten-2-one, **2b**). But in the contrast experiment without AlN shown in the top of Fig. 6a, there is no dehydration product and the content of dimer (**1**) is nearly halved in quantitative determination compared with the additive of AlN. So the nanosized AlN not only promotes dimerization of

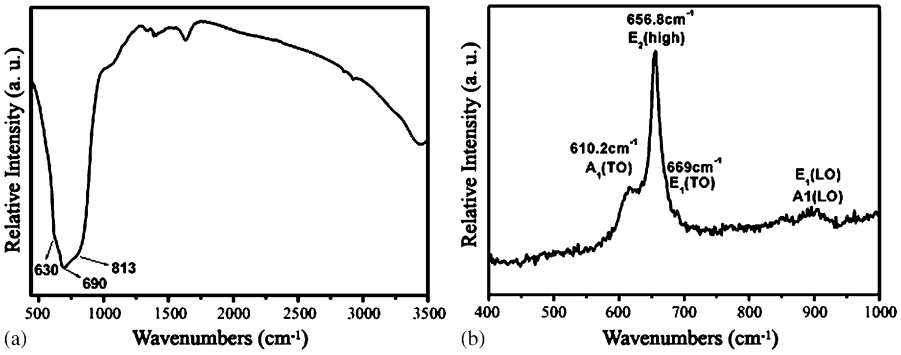

Fig. 5. (a) The IR spectrum of as-obtained AlN nanowhiskers. (b) Raman spectrum of as-prepared AlN nanowhiskers.

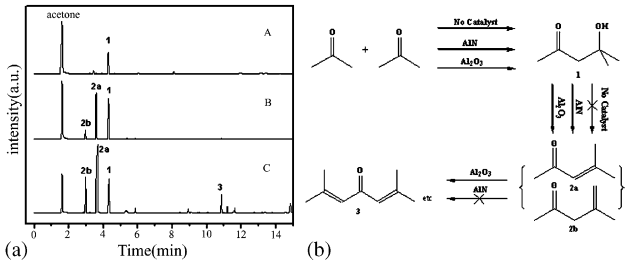

Fig. 6. (a) The chromatogram spectrum of the products in the absence of AlN and Al_2O_3 (A), and in the additives of AlN (B), Al_2O_3 (C), respectively. The 1, 2a, 2b, 3 marked above the peaks represent 4-methyl-4-hydro-2-pentanone, 4-methyl-3-penten-2-one, 4-methyl-4-penten-2-one, 2,6-dimethyl-2, 5-Heptadien-4-one, respectively. The unmarked peaks in C after 5 min are the other trimers and higher polymers of acetone. (b) The whole catalytic process: Without the catalyst, there is only 4-methyl-4-hydro-2-pentanone (1) can be obtained; with the additive of AlN, 4-methyl-3-penten-2-one (2a); 4-methyl-4-penten-2-one (2b) can be obtained; when Al_2O_3 was introduced into this system, there are trimers (2,6-dimethyl-2, 5-Heptadien-4-one (3), etc.) and higher polymers of acetone can be found in the final products, besides the above products.

acetone, but also initiates dehydration reaction, acting as a typical Lewis acid catalyst. Our further investigation found that when it was displaced by nanosized Al_2O_3, the condensation solution of the product was complicated (bottom, Fig. 6a), with immergence of various dehydrates of trimers and higher polymers of acetone, such as 2,6-dimethyl-2, 5-Heptadien-4-one (**3**). They are formed by further condensation of **1**, **2a** and **2b** which are less active than acetone. All the experiments are summarized in Fig. 6b. In conclusion, as for the reaction of acetone condensation, nanosized AlN can only selectively catalyze bi-condensation of acetone, rather than the further condensation (trimer and higher polymers of acetone), indicating that AlN is a relatively milder Lewis acid catalyst compared with Al_2O_3. These results have the potential to be extended to other Lewis-acid catalysed organic reactions.

4. Conclusions

In conclusion, pure hexagonal AlN nanowhiskers have been successfully synthesized by reacting $AlCl_3$ with the nitrogen sources NaN_3 at a low temperature of 450 °C for 24 h. Here, this is the first report on the preparation of the AlN nanostructures with pure-phase under a relatively low temperature. Furthermore, the study on the corresponding optical properties and catalytic properties are also carried out. Due to its low cost and high efficiency, the method in this work could be recommended for practical AlN nanowhiskers synthesis. Further work is under way to study the properties of these nanowhiskers and the possibility of synthesizing other nitride nanowhiskers.

Acknowledgments

This work was supported by National Natural Science Foundation of China, Chinese Ministry of Education, and Chinese Academy of Science. The authors thank Prof. Shuyuan Zhang, Prof. Fanqing Li for technical assistance in TEM and FE-SEM experiments, respectively. The authors also thank Dr. Shuangzheng Lin for helpful discussion for the catalytical properties.

References

[1] K. Jagannadham, T.R. Watkins, R.B. Dinwiddie, J. Mater. Sci. 37 (2002) 1363.
[2] H. Kitagawa, Y. Shibutani, S. Ogata, Modelling Simulation Mater. Sci. Eng. 3 (1995) 521.
[3] Y. Goldberg, in: M.E. Levinshtein, S.L. Rumyantsev, M.S. Shur (Eds.), Properties of Advanced Semiconducting Materials: GaN, AlN, InN, BN, SiC, SiGe, Wiley, New York, 2001, pp. 31–47.
[4] N. Kuramoto, H. Taniguchi, I. Aso, Am. Ceram. Soc. Bull. 68 (1989) 883.
[5] V. Fuflyigin, E. Salley, A. Osinsky, P. Norris, Appl. Phys. Lett. 77 (2000) 3075.
[6] M. Yu, X. Hao, D. Cui, Q. Wang, X. Xu, M. Jiang, Nanotechnology 14 (2003) 29.
[7] P.G. Caceres, J. Am. Ceram. Soc. Bull. 69 (1994) 1801.
[8] S.M.L. Sastry, R.J. Lederick, T.C. Peng, J. Met. 40 (1988) 11.
[9] L.M. Sheppard, Am. Ceram. Soc. Bull. 69 (1990) 1801.
[10] P.G. Caceres, H.K. Schmid, J. Am. Ceram. Soc. 77 (1994) 977.
[11] J.A. Haber, P.C. Gibbons, W.E. Buhro, Chem. Mater. 10 (1998) 4062.
[12] I.P. Parkin, Chem. Soc. Rev. 25 (1996) 199.
[13] Q. Lu, Q. Hu, K. Tang, Y. Qian, G. Zhou, X. Liu, J. Xing, Chem. Lett. 11 (1999) 1239.
[14] D. Kuang, Y. Fang, H. Liu, C. Frommen, D. Fenske, J. Mater. Chem. 13 (2003) 662.
[15] C.D. Wanger, W.M. Riggs, L.E. Davis, J.F. Moulder, G.E. Muilenberg, Handbook of X-ray Photoelectron Spectroscopy, Perkin–Elmer Corporation, Eden Prairie, 1978.
[16] Z. Li, Y. Xiong, Y. Xie, Inorg. Chem. 42 (2003) 8105.
[17] C.D. Wagner, D.E. Passoja, H.F. Hillery, T.G. Kinisky, H.A. Six, W.T. Jansen, J.A. Taylor, Auger and photoelectron line energy relationships in aluminum–oxygen and silicon–oxygen compounds, J. Vac. Sci. Technol. 21 (1982) 933–944.
[18] E.A. Secco, Can. J. Chem. 40 (1962) 2191.
[19] G.D. Singer, H.J. Mueller, Nature 207 (1965) 1073.
[20] J.A. Dean (Ed.), Lange's Handbook of Chemistry, 13 ed., McGraw-Hill, New York, 1985.
[21] Y. Li, Y. Qian, H. Liao, Y. Ding, L. Yang, C. Xu, F. Li, G. Zhou, Science 281 (1998) 246.
[22] R.A. Janes, M.A. Low, R.B. Kaner, Inorg. Chem. 42 (2003) 2714.
[23] J.P. Xiao, Y. Xie, R. Tang, W. Luo, Inorg. Chem. 42 (2003) 107.
[24] X. Chen, K.E. Gonsalves, J. Mater. Res. 12 (1997) 1274.
[25] H.H. Wang, Mod. Phys. Lett. 14 (2000) 523.
[26] U. Mazur, Langmuir 6 (1990) 1331.
[27] K. Seki, X. Xu, H. Okabe, J.M. Frye, J.B. Halpern, Appl. Phys. Lett. 60 (1992) 2234.
[28] Y.G. Cao, X.L. Chen, Y.C. Lan, J.Y. Li, Y.P. Xu, T. Xu, Q.L. Liu, J.K. Liang, J. Cryst. Growth 213 (2000) 198.
[29] F. Agullo-Rueda, E.E. Mendez, B. Bojarczuk, S. Guha, Solid State Commun. 115 (2000) 19.
[30] M. Kuball, J.M. Hayes, A.D. Prins, N.W.A. van Uden, D.J. Dunstan, Y. Shi, J.H. Edgar, Appl. Phys. Lett. 78 (2001) 724.